

Remote Estimates of Ice Algae Biomass and Their Response to Environmental Conditions during Spring Melt

KARLEY CAMPBELL,^{1,2} CHRISTOPHER J. MUNDY,¹ DAVID G. BARBER¹ and MICHEL GOSSELIN³

(Received 11 June 2013; accepted in revised form 27 January 2014)

ABSTRACT. In this study, we support previous work showing that a normalized difference index (NDI) using two spectral bands of transmitted irradiance (478 and 490 nm) can be used as a non-invasive method to estimate sea ice chlorophyll *a* (chl *a*) following a simple calibration to the local region. Application of this method during the spring bloom period (9 May to 26 June) provided the first non-invasive time series dataset used to monitor changes in bottom ice chl *a* concentration, an index of algal biomass, at a single point location. The transmitted irradiance dataset was collected on landfast first-year sea ice of Allen Bay, Nunavut, in 2011, along with the physical variables thought to affect chl *a* accumulation and loss at the ice bottom. Time series biomass calculated using the NDI technique adhered well to core-based biomass estimates, although chl *a* values remained low throughout the bloom, reaching a maximum of 27.6 mg m⁻² at the end of May. It is likely that warming of the bottom ice contributed to loss of chl *a* through its positive influence on brine drainage and ice melt. Chl *a* content in the bottom ice was also significantly affected by a storm event on 10 June, which caused extensive surface melt and a rapid increase in the magnitude of transmitted irradiance. Furthermore, the velocity of current, measured below the ice at the end of a spring neap-tidal cycle, was negatively associated with ice algae chl *a* biomass (the stronger the current, the less biomass). The NDI method to remotely estimate ice algal biomass proved useful for application in our time series process study, providing a way to assess the effects of changes to the sea ice environment on the biomass of a single population of ice algae.

Key words: ice algae, biomass, sea ice, transmitted irradiance, Arctic, algal blooms

RÉSUMÉ. La présente étude vient appuyer d'anciennes études selon lesquelles un indice par différence normalisée (IDN) recourant à deux bandes spectrales d'éclairement énergétique transmis (478 et 490 nm) peut servir de méthode non invasive d'estimation de la chlorophylle *a* (chl *a*) de glace de mer suivant un simple étalonnage dans une aire locale. Le recours à cette méthode pendant la saison de l'efflorescence printanière (du 9 mai au 26 juin) a permis d'obtenir le premier ensemble de données non invasives en séries chronologiques dans le but de surveiller les changements se manifestant dans la concentration de chl *a* de la glace de fond, un indice de biomasse algale, en un seul point. Les données relatives à l'éclairement énergétique transmis ont été recueillies à partir de la glace de mer de rive de l'année à la baie Allen, au Nunavut, en 2011, en même temps que les variables physiques censées avoir des effets sur l'accumulation de chl *a* et sur la perte de glace de fond. Les données chronologiques relatives à la biomasse calculées à l'aide de la technique de l'IDN cadraient bien avec les estimations de la biomasse obtenues à l'aide d'échantillons, bien que les valeurs de la chl *a* restaient à la baisse pendant l'efflorescence, pour atteindre un maximum de 27,6 mg m⁻² à la fin du mois de mai. Il est vraisemblable que le réchauffement de la glace de fond a entraîné la perte de chl *a* en raison de son influence positive sur l'égouttage de la saumure et la fonte des glaces. La teneur en chl *a* de la glace de fond a également été fortement touchée par un événement pluvio-hydrologique qui a eu lieu le 10 juin, événement qui a entraîné une importante fonte en surface et l'augmentation rapide de la magnitude de l'éclairement énergétique transmis. Par ailleurs, la vitesse du courant, mesurée sous la glace à la fin d'un cycle printanier de marée de mortes-eaux, a été négativement liée à la biomasse en chl *a* de l'algue glaciaire (plus le courant était fort, moins la biomasse était grande). La méthode de l'IDN en vue d'estimer la biomasse de l'algue glaciaire à distance s'est avérée utile dans le cadre de l'application de notre étude en séries chronologiques, car elle a présenté un moyen d'évaluer les effets des changements caractérisant l'environnement de la glace de mer sur la biomasse d'une seule population d'algues glaciaires.

Mots clés : algue glaciaire, biomasse, glace de mer, éclairement énergétique transmis, Arctique, efflorescences algales

Traduit pour la revue *Arctic* par Nicole Giguère.

¹ Centre for Earth Observation Science, Faculty of Environment, Earth and Resources, University of Manitoba, Winnipeg, Manitoba R3T 2N2, Canada

² Corresponding author: umcampb2@myumanitoba.ca

³ Institut des sciences de la mer, Université du Québec à Rimouski, 310 Allée des Ursulines, Rimouski, Québec G5L 3A1, Canada

INTRODUCTION

Ice algae are an important feature of the Arctic marine ecosystem. Their biomass, with chlorophyll *a* (chl *a*) concentrations ranging from 1 to 340 mg m⁻² (Arrigo et al., 2010), provides a concentrated food resource for pelagic and sea ice grazers in early spring (Søreide et al., 2010). Ice algae contribute to marine primary production, extending biological production in polar waters by approximately one to three months (Cota et al., 1991) and providing between 4% and 67% of total primary production (Horner and Schrader, 1982; Legendre et al., 1992). The large range in estimates highlights the regional dependence of their contribution. In the context of the landfast first-year sea ice near Resolute Bay investigated in our study, ice algae contribute approximately 10% of total phytoplankton production (Michel et al., 2006).

Algae using sea ice as a growth substrate are concentrated largely in the bottom 10 cm of first-year Arctic sea ice (FYI; Smith et al., 1990). This habitat positions cells in an optimal location to receive irradiance from above, while providing a permeable sea ice environment with minimal temperature and space variability and access to nutrients from the underlying seawater. Ice algae growth commences once a minimum irradiance threshold for photosynthesis has been reached, around February to March (Gosselin et al., 1985; Cota and Horne, 1989; Welch and Bergmann, 1989; Smith et al., 1990). After that time, algae grow exponentially until a plateau is reached as they transition from limitation of light to nutrient limitation (Gosselin et al., 1990; Lavoie et al., 2005). The bloom ends with the onset of sea ice melt (Lavoie et al., 2005); however, the primary physical mechanisms contributing to biomass variability, and especially to loss of biomass from the ice, remain points of debate. Potential mechanisms include influences of sub-ice structure (Eicken, 1992), ice growth rate (Legendre et al., 1991), brine drainage (Mundy et al., 2007a), physical ice melt and warming rate, light limitation as a function of snow depth, biological melt through heat release by algal cells following transmitted irradiance absorption (Lavoie et al., 2005), and photoinhibition (Rintala et al., 2006).

The concentration of the chl *a* pigment in sea ice is often used as an index of ice algal biomass because the two variables have a reliable positive relationship (Hsaio, 1992). Collection of chl *a* samples is primarily accomplished by ice core extraction followed by lab analysis from subsamples taken after the ice core has melted. This method remains the standard for ice algal chl *a* determination (Horner et al., 1992). However, ice core extraction is time-intensive and can result in loss of algae, particularly during advanced stages of melt (Welch et al., 1988). Furthermore, ice core extraction is destructive, which makes a representative time series of ice algal biomass at a single point location impossible.

The photosynthetic and accessory pigments found in ice algae preferentially absorb light at particular wavelengths, most notably at 440 and 676 nm for chl *a* (Bricaud et al.,

2004). As a result, ice algae alter the spectral distribution of light transmitted through the ice in a way that has been statistically associated with their biomass. The use of wavelength-specific transmitted irradiance to assess biomass was first examined by Legendre and Gosselin (1991) and later improved upon by Mundy et al. (2007b), who accounted for 89% of biomass variability using a normalized difference index (NDI) of wavelengths 485 and 472 nm.

High-resolution time series observations are necessary to understand the ecosystems associated with sea ice (Cota and Smith, 1991). This study addresses such a need by using the standardized transmitted irradiance method developed by Mundy et al. (2007b) to estimate the change in biomass of the same algal community from the end of the cold season through the peak of the spring bloom to its termination in the landfast FYI of the Canadian High Arctic. Coincident physical variables were also sampled to examine the biophysical processes affecting algal biomass accumulation and loss over this period. This paper presents a true time-series study of the ice algae spring bloom and its response to environmental factors during melt.

MATERIALS AND METHODS

Study Site

An ice camp was established on landfast FYI in Allen Bay, northwest of Resolute Bay, Nunavut, Canada (74°43.165' N; 95°10.099' W; Fig. 1). Measurements for this time series assessment were taken in the surrounding area from 9 May to 26 June 2011, as part of the Arctic–Ice Covered Ecosystem (Arctic–ICE) program. The sampling region consisted of smooth ice 1.3–1.7 m thick with a water depth of ~60 m in the bay. During the sampling period, air temperature ranged from –15.9 to 6.6°C, and the sea ice surface evolved from snow depths of 5.5 to 50 cm in mid-spring to white ice (*sensu* Maykut and Grenfell, 1975) and melt pond cover toward the end of the study. Ice break-up occurred immediately after this study on 28 June 2011.

Transmitted Irradiance Measurements

From 9 May to 26 June, the spectral distribution of incident downwelling irradiance 1 m above the snow surface ($E_d(0, \lambda)$) and downwelling irradiance transmitted 15 cm beneath the ice–water interface ($E_d(z, \lambda)$) was measured every day between 0900 and 1200 at a time series site (74°43.110' N; 95°10.077' W) and once every four days at core locations. Both spectra were measured simultaneously from 350 to 1050 nm with a 1.4 nm bandwidth using a dual head VIS-NIR spectrometer (Analytical Spectral Devices Inc.) equipped with a reverse cosine receptor (RCR; 180° field of view). Deployment of the under-ice RCR largely followed the method described by Mundy et al. (2007b); the sensor head was fixed to an underwater arm placed

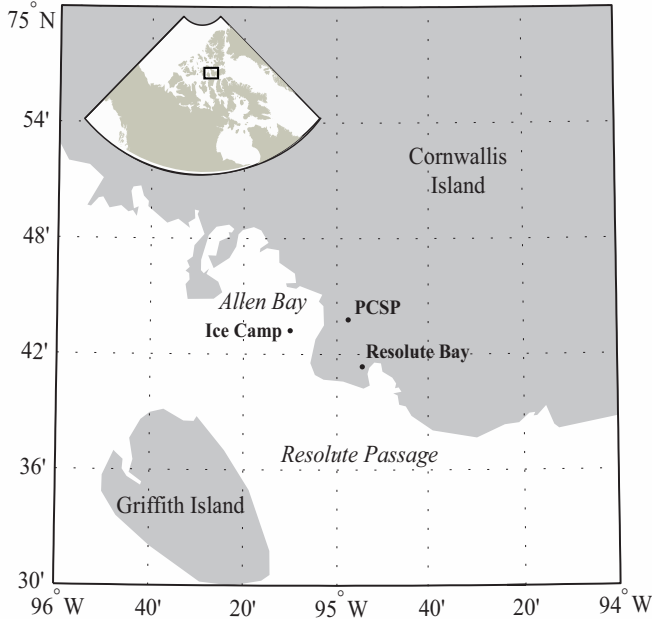


FIG. 1. Location of 2011 Arctic-ICE Allen Bay ice camp (74°43.165' N; 95°10.099' W) relative to the neighbouring community of Resolute Bay and the Polar Continental Shelf Program (PCSP) research station.

perpendicular to the surface 1.5 m south of the auger hole. To minimize light contamination, an opaque foam cover was placed within the auger hole and removed only to insert the sensor.

Spectra recorded using the underwater-calibrated sensor were integrated over 4.35 seconds and surface values were integrated over 17 ms to avoid saturation. A total of five spectra were recorded per measurement, and dark currents were subtracted intermittently during sampling to remove instrument noise. The sensors of the spectrometer were calibrated before use, permitting the automatic recording of irradiance in $\text{W m}^{-2} \text{nm}^{-1}$ during fieldwork.

Deriving Time Series Chl *a* from $E_d(z, \lambda)$

Time Series Sampling: Daily measurement of transmitted irradiance at the time series location required care to avoid site disturbance. For example, during the first half of the study, a surface layer of ice would form overnight, and therefore the hole had to be re-excavated on the next visit. Extreme caution had to be taken when operating the auger so as not to flood the time series site or have ice shavings fall on it. Unfortunately, this daily removal and re-deployment of the sensors could not be avoided, as the sensors were required for measurements in addition to our time series. Following measurement of transmitted irradiance, we recorded an average of five snow depths on a similar snow cover 1 m east of the irradiance sampling area (to avoid disturbance). Averaging of five snow depths was also accomplished at core locations (see Core Sampling below) following the measurement of $E_d(z, \lambda)$ and prior to ice core extraction.

Core Sampling: Every fourth day, new coring locations were established at sites representing each of the ice surface conditions present. During the early spring this included three snow categories: low (L; < 10 cm), medium (M; 10 to 18 cm), and high (H; > 18 cm) depths. Later, during advanced melt, these categories shifted to melt ponds (L) and snow or drained white ice (H). Measurements at melt ponds were considered extensions of the low snow depth category into the late spring because ponds are predisposed to form between drifts at low snow depth sites (Iacozza and Barber, 1999). Similarly, the persistence of snow or presence of white ice was assumed to indicate prior locations of high snow depths. At these locations, $E_d(z, \lambda)$ was measured according to the method described for transmitted irradiance before two ice cores were extracted using a 9 cm Mark II Kovacs coring system.

The bottom 10 cm of each site's cores were combined with filtered seawater at a ratio of three parts filtered seawater to one part ice core volume, then melted slowly in the dark to minimize osmotic stress (Garrison and Buck, 1986) and exposure to rapid changes of in situ light levels (Arrigo et al., 2010; Juhl and Krembs, 2010). Once the core sample was melted (after approximately 18 to 24 hours), a pseudo-replicate set of subsamples was filtered onto Whatman GF/F filters. After placing the filters in 10 ml of 90% acetone for 18 to 24 hours, fluorometric measurements of chl *a* were taken using a Turner Designs Fluorometer 10-005R before and after acidification with 5% HCl (Parsons et al., 1984). Areal chl *a* concentration was calculated from these measurements using the equation of Holm-Hansen et al. (1965).

Calculation of Time Series Biomass: Following Mundy et al. (2007b), Pearson correlation surfaces between NDI values and core-based chl *a* were determined for all possible NDIs:

$$\text{NDI} = [E_d(z, \lambda_1) - E_d(z, \lambda_2)] / [E_d(z, \lambda_1) + E_d(z, \lambda_2)] \quad (1)$$

and therefore for all wavelength combinations of transmitted irradiance and core-based chl *a* data. Correlation values calculated from wavelengths greater than 700 nm were noisy; therefore, only wavelengths of photosynthetically active radiation (PAR; wavelengths 400–700 nm) were used. Chl *a* concentrations (in mg m^{-2}) at the time series site were calculated using a linear least squares regression fit of the core-based chl *a* concentrations versus the highest correlated NDI.

Physical Sampling

In addition to snow depth, other environmental factors that potentially influence ice algae biomass were investigated. The transmittance of integrated PAR wavelengths (Tr_{PAR}) through the sea ice, which is the ratio of $E_d(z, \lambda)$ to $E_d(0, \lambda)$, was determined at the time-series site with the VIS-NIR spectrometer. For convenience, in the present study Tr_{PAR} is expressed as a percentage. The meteorological tower

maintained near the ice camp (74°42.850' N, 95°11.980' W) was fitted with a Campbell Scientific CR23X data logger that recorded one-minute averages of the following measurements: incident downwelling PAR (Kipp & Zonen PAR-Lite; 1 second sampling interval), later integrated over PAR wavelengths and defined as $E_d(0, \text{PAR})$; air temperature (Vaisala HMP45C212; 1 second sampling interval); wind speed (RM Young 05103 anemometer; 2 second sampling interval); and ice temperature (Type T thermocouples; 2 second sampling interval). A bottom ice temperature gradient (TG; °C m⁻¹) was calculated from measurements recorded at depths 0.6 (T_{0.6 m}) and 1.2 m (T_{1.2 m}) below the air-ice interface:

$$\text{TG} = (T_{1.2\text{ m}} - T_{0.6\text{ m}}) / 0.6 \text{ m} \quad (2)$$

and was linearly corrected for instrument error prior to 24 May.

Alongside coring for chl *a* analysis, an additional core was taken at the medium snow depth category (high category during the melt period) site to measure sea ice thickness and temperature (Testo 720 probe) at 10 cm intervals, and salinity (WTW 330i conductivity meter) for 10 cm sections. These values were later used to calculate percent brine volume, following the equations of Cox and Weeks (1983). Brine volumes were averaged for the entire ice profile and reported as average brine volume (BV_{AVG}). Because of sampling time restrictions, cores used to calculate these values were collected only every four days.

Current velocity (cm s⁻¹) at 2.5 m below the air-ice interface was monitored at a nearby site (74°43.103' N, 95°10.031' W) using an ALEC Infinity-EM current meter tethered to the sea ice. Current velocities were averaged over 24-hour periods to obtain the mean daily current velocity (hereafter CV_{AVG}) for each sample day.

Principal Component Analysis

A principal component analysis (PCA) (Pielou, 1984; Gotelli and Ellison, 2004) was performed to explore the relationships between environmental factors (snow depth (H_s), $E_d(0, \text{PAR})$, Tr_{PAR}, TG, and CV_{AVG}) and NDI-estimated chl *a* throughout the study period.

RESULTS AND DISCUSSION

Site Conditions

Air temperature remained below 0°C, warming from -15.9°C on 9 May to -0.14°C on 14 June. During this period, snow depth at the time series site ranged from 10.8 to 20.4 cm and averaged 16.2 cm, thus classifying it as a medium-depth site. The characteristics of the sea ice surface quickly transitioned during a storm weather event on 10 June, which brought rainfall and strong northeastern winds increasing to 17.5 m s⁻¹. Site conditions after the

storm were characterized by a thin snow cover and eventually white ice. A rapid decrease in snow depth corresponded to a rise in Tr_{PAR} at the time series site (Fig. 2) as well as an albedo decline from averages of 0.83 (10 June and earlier) to 0.41 (11 June and later) at the nearby meteorological tower (data not shown). Over the course of 10 June alone, albedo changed from 0.66 to 0.40. These large differences are a consequence of rapid snowmelt as larger snow grains—and ultimately the exposed ice surface and meltwater—permitted greater transmission of incoming radiation into the ice instead of reflecting it back to the atmosphere (Perovich et al., 1998; Mundy et al., 2005). From 15 June to the end of sampling on 26 June, air temperatures stayed above 0°C.

Optimal NDI

The correlation analysis between all possible NDI wavelength combinations and ice core chl *a* concentrations measured under high, medium, and low snow cover is presented in Figure 3. The regression analysis was based on the data from high, medium, and low calibration sites grouped together because no significant difference between snow depth categories was found (Chow Test; $p > 0.05$). In this assessment, the wavelength combination of 478 and 490 nm demonstrated the strongest correlation with $r = 0.90$ and accounted for 81% of chl *a* variability following regression analysis. Application of the Mundy et al. (2007b) NDI, which used wavelengths 472 and 485 nm, accounted for 79% of core chl *a* variability in this study. Subsequently, biomass calculated using wavelengths 472 and 485 did not differ greatly from values calculated using wavelengths 478 and 490 nm (root mean square error = 2.2, $n = 41$). Therefore, either combination of wavelengths, 478 and 490 or 472 and 485, could have been used as a reliable and relatively robust estimator of ice algae biomass. Following the recommendation of Mundy et al. (2007b) to calibrate NDIs regionally, and because of its correlation ranking, an NDI using wavelengths 478 and 490 (hereafter NDI_{478/490}) was chosen as the best representation of algae biomass and was used for chl *a* calculation in this study.

Despite the similarity in NDI wavelengths and predictability power of the algorithms, the regressions of core chl *a* and NDIs in our study (see equation 3) and in Mundy et al. (2007b) were statistically different (Chow Test, $p < 0.05$). A deviation in slope suggests differences in algal photophysiology, such as changes to chl *a*-specific absorption coefficients or the presence of packaging effects.

Average chl *a* measured by Mundy et al. (2007b) in 2003 in the Resolute Bay area was 30.6 mg m⁻², reaching a maximum concentration of 109 mg m⁻². In contrast, the 2011 biomass was half the 2003 average at 16.8 mg m⁻² and only reached a maximum biomass of 22.1 mg m⁻² during the same period. Higher concentrations of chl *a* and therefore algal biomass can lead to shading of algae lower in the ice column (Robinson et al., 1995), resulting in stronger absorption in the 450–550 nm region through production of the accessory pigment fucoxanthin (SooHoo et al., 1987).

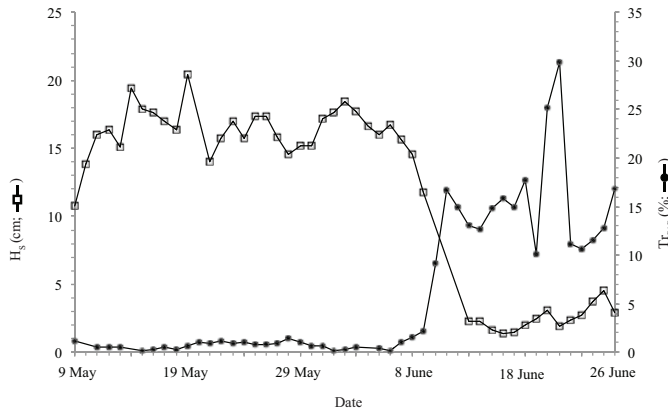


FIG. 2. Changes in snow depth (H_s , \square) and PAR transmittance (Tr_{PAR} , \bullet) at the time-series site from 9 May to 26 June. Values after 10 June represent the depth of white ice.

This possibility suggests that calibration of $E_d(0, \lambda)$ estimates is especially recommended when measuring algae populations of different relative biomass.

Furthermore, sampling in our study extended longer into the spring melt period by 34 days, which means that different environmental conditions were experienced by the ice algae. During later melt stages, ice algae can change their physiological state from shade-acclimation (high photosynthetic carotenoids to chl a ratio) to photoprotection (high photoprotective carotenoids to chl a ratio) (Alou-Font et al., 2013). Preliminary pigment analysis on data collected during the 2011 Resolute campaign support this hypothesis, as the ratio of photoprotective to photosynthetic carotenoids increased with a large rise in transmitted irradiance following the 10 June storm event (Blais et al., 2012). A change in these pigment compositions could directly affect the wavelength bands used as the optimal NDI in our study as the most abundant diatom photosynthetic carotenoid, fucoxanthin, has a broad absorption peak from 490 to 515 nm, whereas the important photoprotective carotenoid, diadinoxanthin, has a sharp peak centered at ~ 490 nm (Bricaud et al., 2004).

Time Series Chl a Calculation

Time series chl a concentration (Fig. 4) was calculated from the linear regression between NDI_x and core-based chl a concentration:

$$\text{chl } a \text{ (mg m}^{-2}\text{)} = (-497.2 \times (NDI_x) + 15.2) \quad (3)$$

The root mean squared error calculated for NDI_x -derived chl a and core chl a data was low at 3.73 ($n = 41$). The predictability power of chl a from NDI measurements is therefore a reliable proxy of measurement for ice algae biomass. However, the presence of some negative chl a values following the use of equation 3, a result of its calibration to core-based chl a , highlights an additional error. Therefore, it is stressed that this method is not meant to replace ice core sample collection, but to provide a remote sensing tool

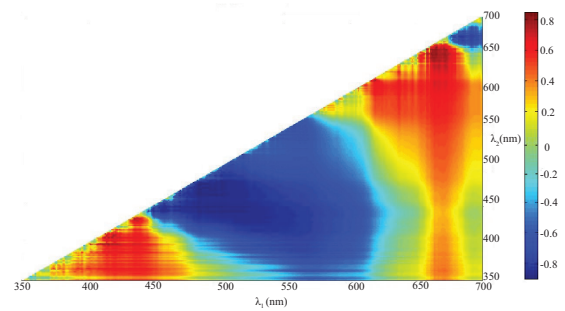


FIG. 3. Pearson correlation surface of all possible normalized difference indices (NDIs) with core-derived chlorophyll a (chl a) measurements.

that can increase spatial and temporal coverage of regional measurements.

Biomass calculated for the time series location is presented in Figure 5. For the purposes of this study, negative NDI biomass estimates were assigned values of 0 mg m^{-2} for analyses. Time series values of calculated biomass indicated a chl a increase until 13 May, after which biomass oscillated between 10.3 and 23.9 mg m^{-2} until reaching the peak chl a concentration on 6 June at 27.6 mg m^{-2} (Fig. 5). Biomass declined sharply thereafter, becoming lower than any prior biomass on 10 June, until reaching 0 mg m^{-2} on 14 June. Subsequent chl a concentrations fluctuated between 0 and 8 mg m^{-2} . The length of the time series therefore resulted in a full description of the ice algae bloom, its increase to peak biomass, and its decline to bloom termination.

With the exception of measurements during the advanced melt period, calculated chl a values adhered well to core-based estimates under medium snow depths (Fig. 5). The maximum time series biomass of 27.6 mg m^{-2} was below the lower range of chl a concentrations previously reported for the region, which range an order of magnitude between 35 (Fortier et al., 2002) and 250 mg m^{-2} (Smith et al., 1988). Maximum chl a in our study was more similar to that observed in nearby Jones Sound by Apollonio (1965), who reported maximums of approximately 23 mg m^{-2} in both 1962 and 1963. Large inter-annual differences in ice algae biomass are not uncommon for the Canadian Archipelago and are thought to be a result of variability in the nutrient content of inflowing waters of Pacific origin (Michel et al., 2006). Rózanska et al. (2009) further demonstrated a significant positive relationship between maximum algae biomass in landfast first-year sea ice and early spring surface nitrate concentrations. Thus, the low estimates of chl a in our study could have been influenced by nutrient limitation. Despite these differences in bloom magnitude, the timing of bloom peak on 25 May, as determined from the fitting of time series biomass with a second order polynomial (values beyond 13 June not included; $y = -0.0419x^2 + 12.1x - 854.9$; $r^2 = 0.561$), closely matched that of previous studies (e.g., Smith et al., 1988; Lavoie et al., 2005). The specific date at which ice algae blooms reach zero biomass is often undocumented, which highlights the

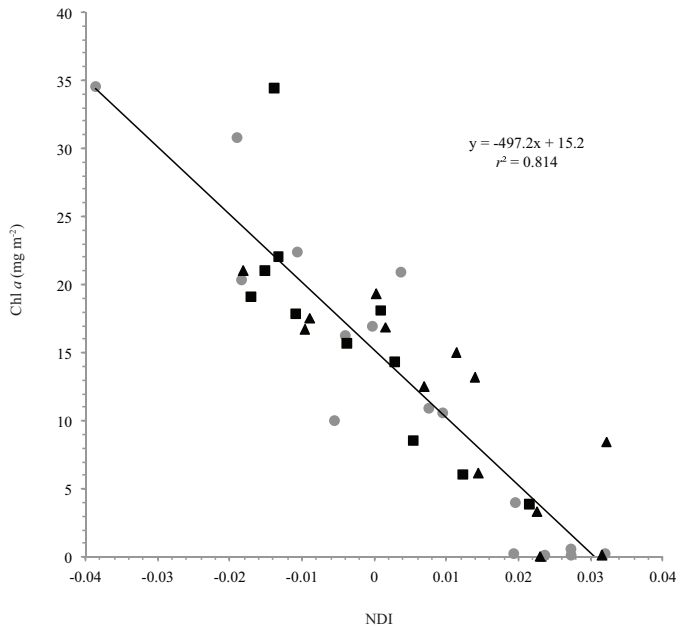


FIG. 4. Regression between core-based chlorophyll *a* (chl *a*) and normalized difference indices (NDIs) measured at the same location ($p < 0.01$) under high (●), medium (■) or low (▲) snow depths.

significance of our time series measurements. Comparison of the 14 June bloom termination date in this research to extrapolated values in the literature supports the findings of Smith et al. (1988), who suggest that biomass near Resolute Bay would have reached zero around 8 June. These dates, however, are at least one week earlier than the majority of approximated termination dates (20 June or later, e.g., Welch and Bergmann, 1989; Michel et al., 1996; Lavoie et al., 2005). Differences in bloom termination dates may represent interannual variability of spring warming.

The large fluctuations in biomass within short periods of time seen in Figure 5 can be attributed to spatial variability. Small-scale variability of ice algae biomass, capable of changing within 1–30 mm at the ice-ocean interface (Mundy et al., 2007a), could not be captured with the transmitted irradiance methodology used in this study because repositioning of the sampling arm at the exact position between measurements was not possible. Unknowingly placing the sensor under different biomass patches within the same greater sampling region, on the order of 10 cm, could have caused fluctuations in NDI chl *a* estimates and contributed to the time series biomass variability observed in Figure 5. Furthermore, the presence of phytoplankton under sea ice during late spring (e.g., Fortier et al., 2002; Mundy et al., 2009; Arrigo et al., 2012), as well as the observed aggregates of ice algae sloughed from the ice between the sensor and ice interface, would falsely increase biomass estimates of the bottom ice chl *a*.

Use of the transmitted irradiance technique during times when absorption by biological materials immediately below the sea ice is high may therefore be problematic for obtaining accurate biomass estimates unless their origin (ice or water column) can be accounted for (e.g., a camera could

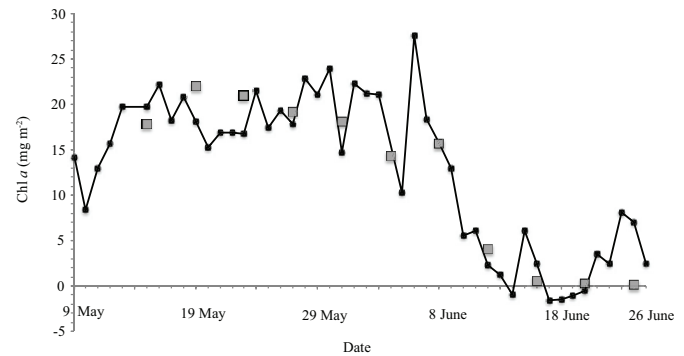


FIG. 5. Changes in chlorophyll *a* (chl *a*) concentration at the time-series site (calculated values, ●) and at high snow depth core locations (measured values, ■) from 9 May to 26 June.

help distinguish between ice algae and floating algal aggregates). Limitations of the method during advanced melt were also highlighted by the presence of negative biomass values, which may further restrict its use and reliability during this period and in general in regions of low ice algal biomass.

Environmental Influences on Ice Algae Biomass

Principal Component Analysis: The results of the PCA analysis are displayed in Figure 6, using components 1 and 2 as *x* and *y* axes, which together accounted for 84.41% of data variability, the majority of which was described by component 1 (eigenvalue (χ) = 4.07, 66.85%). Data points on this figure represent the different days on which data for chl *a*, Tr_{PAR} , CV_{AVG} , TG, $E_d(0, PAR)$, and snow depth (H_s) variables, depicted as vectors, were collected. Only variables with daily sampling frequency were used in this analysis and thus, BV_{AVG} was not included.

Data points formed two distinct groups along the axis of component 1: days prior to the 10 June storm event (on the lefthand side) and those after (on the righthand side). Days with missing data for any one of the variables were excluded in the PCA analysis. As a result of missing H_s data, points for 11–13 June are not present in Figure 6, a factor that may have contributed to the gap observed between groups. Nevertheless, values of bottom ice chl *a* concentration and all environmental variables except $E_d(0, PAR)$ changed significantly following the spring storm, an observation supported by the field observations discussed under “Site Conditions” above. The position of sample days relative to vectors indicates that the time series site before 10 June had higher bottom ice chl *a* biomass in a snow-covered, low-light environment with lower ice temperatures and weaker tidal currents, while the opposite trend was observed after 10 June. Fortier et al. (2002) observed a rapid loss of ice algae from the sea ice following rain events and warm spells similar to that observed in our study. Our results agree with these findings, suggesting that single weather events can have large effects on the physical FYI environment and subsequently on ice algae. In particular, the ice algae bloom may experience earlier termination and overall suppressed

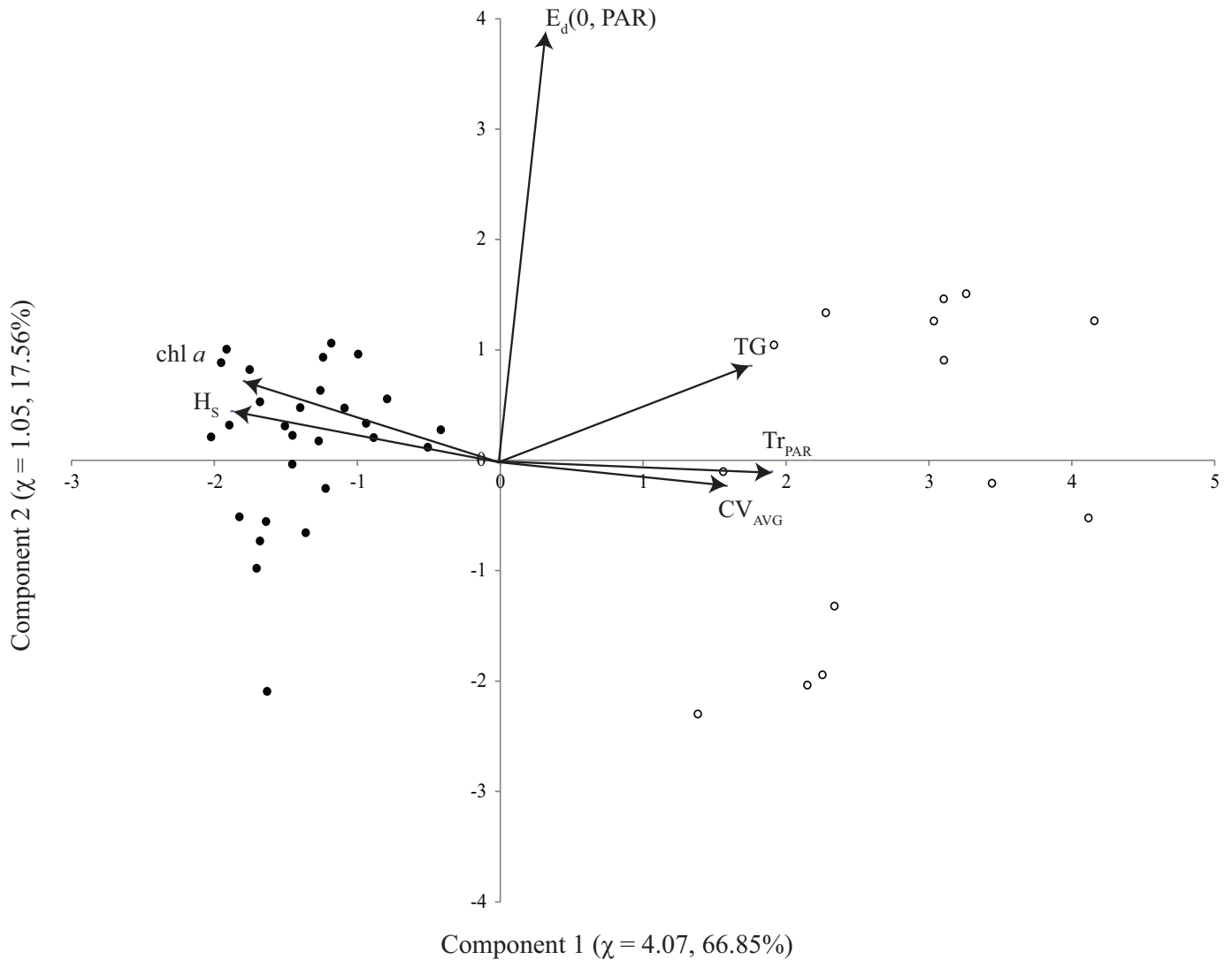


FIG. 6. Principal component analysis of variables sampled on the landfast ice of Allen Bay (Nunavut) from 9 May to 9 June (●) and from 10 to 26 June (○). The environmental and biological variables are snow depth (H_s), surface integrated PAR ($E_d(0, \text{PAR})$), PAR transmittance (Tr_{PAR}), temperature gradient between 60 to 120 cm from the ice surface (TG), mean daily current velocity at 2.5 m below the air-ice interface (CV_{AVG}), and calculated bottom ice chlorophyll a (chl a) concentration.

biomass accumulation with the rapid removal of snow that these storms cause (Campbell et al., 2014). The anticipated increase in frequency of storm events in the Arctic likely represents a negative impact of climate change on ice algae, and therefore the marine environment, considering the dependence of higher trophic levels on the presence and timing of the ice algae bloom (Leu et al., 2011).

The largest contributors to point spread over PCA component 1 were Tr_{PAR} and H_s , which were negatively associated with each other. These observations demonstrate the strong influence of snow on light transmission, which has been theoretically shown to impact algal biomass loss via physical (and to a much lesser extent, biological) melt processes (Lavoie et al., 2005), as well as through its control on algal photosynthesis (Gosselin et al., 1986). The negative or positive association between Tr_{PAR} (H_s) and chl a supports previous observations in the region and was associated with the progression of the melt period. The vector of

$E_d(0, \text{PAR})$ was nearly parallel with the axis of component 2. Therefore, the broad distribution of points along this axis was a result of variable magnitudes of downwelling PAR over the entire sample period. This outcome represents the variability associated with daily changes in cloud cover and weather conditions, and illustrates that $E_d(0, \text{PAR})$ is not a good predictor of the ice algal bloom decline.

Linear Regression Analysis: To further assess biophysical relationships, linear regressions were performed between environmental variables and associated NDI_x -based estimates of chl a at the time series site (Fig. 7; Table 1). This analysis resulted in two point clusters for variables H_s and Tr_{PAR} when plotted against chl a , which did not permit linear statistical analysis over the entire sample period. Therefore, data were examined as two separate groups based on the division seen in Figure 7a, which corresponded to the separation of points noted following PCA analysis: before and after 10 June.

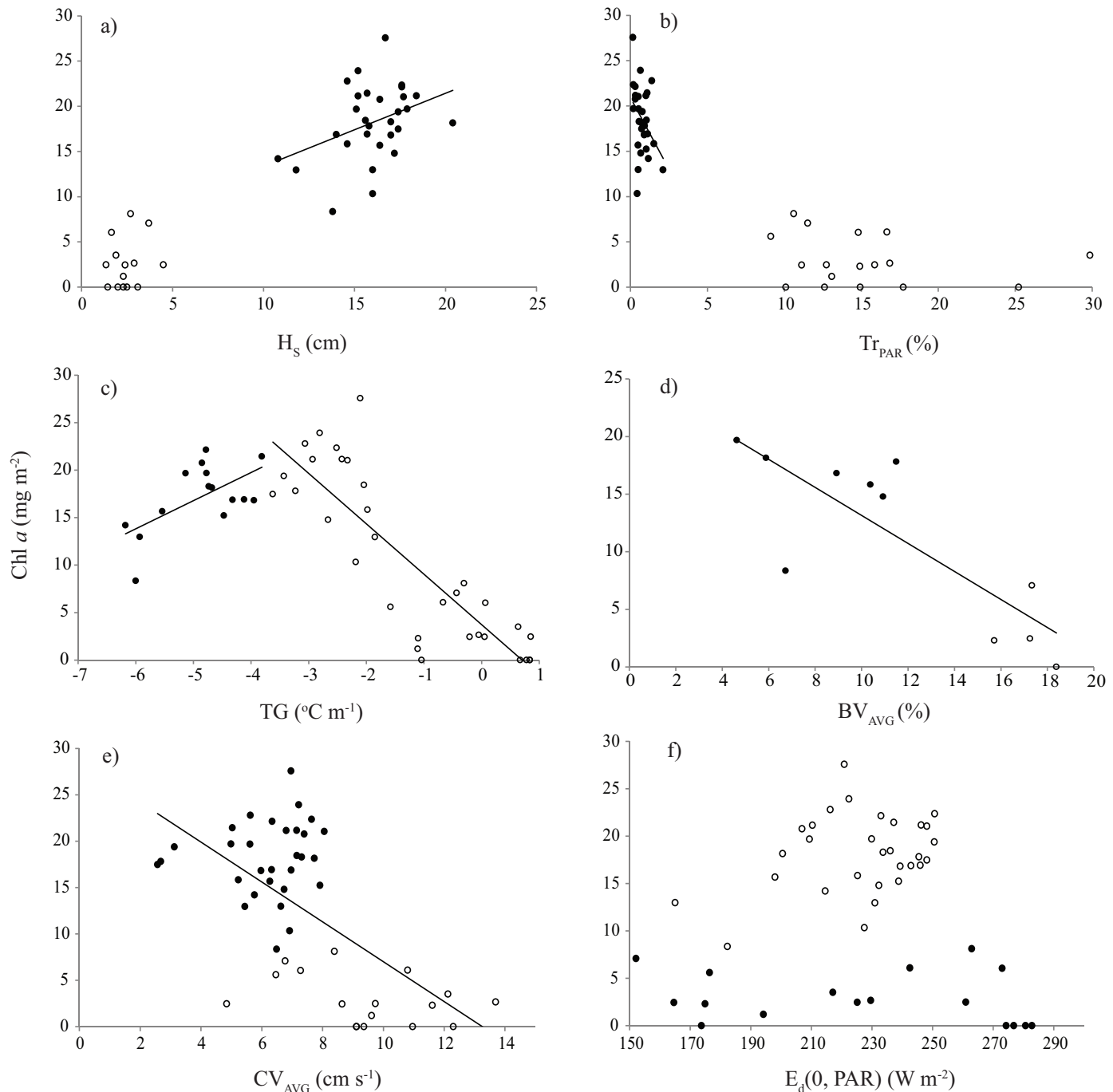


FIG. 7. Relationships between calculated chlorophyll *a* (chl *a*) concentration and a) snow depth (H_s), b) percent PAR transmittance (Tr_{PAR}), c) temperature gradient between 60 to 120 cm from the ice surface (TG), d) average percent brine volume of total ice thickness (BV_{AVG}), e) mean daily current velocity at 2.5 m below the air-ice surface (CV_{AVG}), and f) surface downwelling PAR irradiance ($E_d(0, PAR)$) through (●) and after (○) 9 June. Note that in c), the data are presented before (●) and after (○) 25 May.

The strong negative relationship between snow depth and the magnitude of transmitted irradiance through sea ice has been well documented (Perovich, 1996; Belzile et al., 2000; Mundy et al., 2007b) and is also shown in Figures 2 and 6. The large division of H_s and Tr_{PAR} data around the 10 June storm in Figure 7 (a and b) illustrates the role of snowmelt (and the subsequent increase in PAR transmittance) as a principal variable in determining the start of biomass decline and therefore bloom duration (Gosselin et al., 1986; Lavoie et al.,

2005). This argument is supported by the fact that chl *a* drops below the previous range of variability on 10 June (Fig. 5).

A second-order polynomial fit of chl *a* versus TG ($y = -0.9194x^2 - 7.2193x + 4.5335$; $r^2 = 0.709$, $p < 0.05$) had a peak at $-3.93^\circ\text{C m}^{-1}$. As a result, data were grouped together on each side of this point (9 to 23 May and 24 May to 26 June) for calculation of linear regressions (Fig 7c). During the latter period, a significant negative relationship between biomass and TG was observed, in which chl *a*

TABLE 1. Coefficients of determination (r^2 values) between calculated chl a concentration and environmental variables for three sampling periods: early spring (9 May to 9 June, but 9 to 24 May for TG), late spring (10 to 26 June, but 25 May to 26 June for TG) and the total sampling period (9 May to 26 June) when point distributions permitted statistical analysis. Bolded values are significant at $p < 0.05$.

Variable	Early Spring		Late Spring		Total Period	
	r^2	n	r^2	n	r^2	n
H_S	0.141	29	0.039	14	–	–
Tr_{PAR}	0.140	29	0.047	17	–	–
TG	0.306	15	0.740	32	–	–
BV_{AVG}	0.065	7	0.042	4	0.669	11
CV_{AVG}	0.006	30	0.131	17	0.387	47
$E_d(0, PAR)$	0.097	30	0.043	17	0.000	47

decreased as the ice became increasingly isothermal ($r = 0.740$, $p < 0.05$; Table 1). Warming of the bottom ice can negatively affect ice algae biomass by causing a) ice ablation, resulting in the sloughing of algae from the ice into the water column (Lavoie et al., 2005) or b) brine drainage, which causes algal sloughing following erosion of the ice habitat, particularly where liquid brine drains from the ice (Lavoie et al., 2005; Mundy et al., 2005; Juhl and Krembs, 2010).

Although observations support a small decrease in sea ice thickness at core locations over the sampling period (Fig. 8), the decline was not significant ($r = 0.517$, $p = 0.085$). Ice thickness at the time series location was not assessed because of complications associated with maintaining a time series; the site could not be disturbed for thickness measurements, and estimates from the maintained auger hole would not have been accurate. The influence of bottom ice melt on removal of algal cells, particularly the influence of changes in thickness to the bottom skeletal layer, could not be assessed in this study.

Free movement of brine through sea ice by interconnecting brine pockets and channels has been modelled and observed to occur once the ice approaches -5°C , which corresponds to approximately 5% brine volume in first-year columnar sea ice (Golden et al., 1998; Pringle et al., 2009). In this study, brine volume averaged over the entire ice thickness was above the 5% threshold for the entire sampling period, with the slight exception of brine volume on 27 May at 4.6%. BV_{AVG} remained close to the 5% threshold ($\pm 1.7\%$) until 4 June, after which it increased to a plateau between 10.4% and 11.5%, before a final rise following 8 June that peaked at 18.4% (Fig. 8).

The plot of chl a versus BV_{AVG} had a distribution of points similar to that of H_S and Tr_{PAR} , separated around the 10 June weather event (Fig. 7d). The two BV_{AVG} groups of data represent (left) early spring, when sea ice held lower volumes of brine and supported a larger ice algal community, and (right) late spring during advanced stages of melt, when large volumes of brine and low chl a was measured in the sea ice. Severe weather events therefore have the capacity to cause rapid change not only in the surface ice environment, but also in the internal characteristics of the sea ice.

The decline in the bottom ice salinity over time ($r = 0.855$, $p < 0.05$) shows that gravity-driven drainage of brine from the ice (i.e., brine drainage) and replacement by less

saline meltwater likely occurred (Fig. 8). Theoretically this mechanism of brine drainage, inextricably linked with ice temperature, can contribute to biomass loss (see Gradinger et al., 1991) through interior ice melt of the algal substrate, mechanical erosion of the algal cells by enhanced brine channel flow during drainage, or both. Although the influence of each mechanism on the removal of algal cells could not be differentiated with our dataset, our findings illustrate that the mechanism of brine drainage may have contributed to biomass variability, especially late in the spring (Table 1; Fig. 7d).

Brine flushing, different from brine drainage in that the movement of brine is aided by a meltwater hydrostatic head, has been suggested as a greater contributor to biomass loss during advanced stages of the spring bloom than either melt (biological or physical) or nutrient concentration influences (Lavoie et al., 2005). A drop in salinity throughout the ice column is indicative of flushing events (Polashenski et al., 2012) as brine is replaced by less saline meltwater and ocean water. Analysis of salinity profiles measured from ice cores over the season did not show a similar result (data not shown), indicating that a brine flushing event did not occur during the sampling period.

The validity of a -5°C brine threshold in FYI described by Golden et al. (1998) was questioned by Polashenski et al. (2012) when they found a six-week delay between its onset and flushing by meltwater percolation. In their research, a layer of refrozen meltwater within the upper layer of ice persisted beyond the -5°C mark causing a delay in bulk ice permeability that could translate into postponement in the increase of bulk ice salinity, and therefore of algae removal by means of brine flushing. A similar result to that observed by Polashenski et al. (2012) may thus explain why a brine flushing mechanism was not detected here even though the bulk brine volume of sea ice was equal to or above the percolation threshold.

The increase in chl a during early spring, corresponding to the period with lowest ice temperatures and greatest absolute TG, may have been a result of coincident timing with or a response to changing ice temperatures (Table 1; Fig. 7c). Sampling began during the accumulation phase of the ice algae bloom, so biomass increases were concurrent with, but did not necessarily result from, rising ice temperatures. Alternatively, the significant early spring trend may have represented a temperature gradient threshold

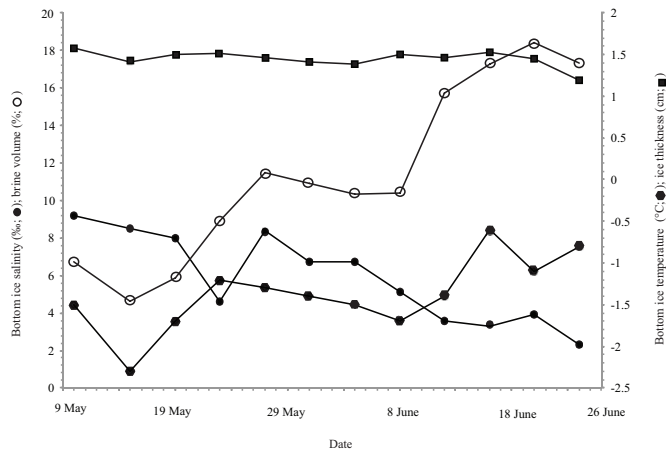


FIG. 8. Changes in temperature (T_{10} ; ●) and salinity (S_{10} ; ○) in the bottom 10 cm of sea ice, average percent brine volume of the entire ice column (BV_{AVG} ; ●), and average ice thickness (■) at medium core locations from 9 May to 24 June measured at medium snow depth core locations.

in the ice at which algae found optimal conditions at the ice subsurface. Ice algae are able to grow at ice temperatures as low as -20°C because of physiological adaptations (Morgan-Kiss et al., 2006) and at temperatures much higher than those recorded in this study (Morgan-Kiss et al., 2002). As a result, instead of physiological responses, temperature-induced changes to algal habitat would have been a more likely influence on biomass. For example, small levels of ice growth during the early spring can increase nutrient supply by creating turbulence at the ice interface following brine rejection (Cota et al., 1991). This positive influence on biomass would have ended when ice growth ceased as a result of warming ice temperatures.

A fortnightly tidal cycle was apparent over the sample period as observed through the plotting of under-ice current velocity over time (data not shown). Increasing currents during periods of the tidal cycle have a significant influence on vertical mixing in waters under the landfast ice-covered region of Resolute Passage (Marsden et al., 1994). These currents can have competing influences on ice algal biomass, causing either increases associated with enhanced nutrient supply (Cota et al., 1991), or decreases due to enhanced bottom ice melt (Lavoie et al., 2005) and mechanical removal of cells (Mundy et al., 2007a). In this study, the removal of algae by currents was supported, as chl *a* was negatively correlated with under-ice current velocity ($r = 0.622$, $p < 0.05$); however, the specific mechanism of biomass loss was not addressed in this research.

SUMMARY AND CONCLUSIONS

The NDI using two spectral bands of transmitted irradiance was a reliable and relatively robust estimator of ice algae biomass, and its use in this research permitted truly non-invasive time-series measurements of ice algae biomass. Future applications of this technique may consider

application of band-specific or multispectral radiometers as a cost-effective means of monitoring biomass over a number of areas. Furthermore, use of radiance measurements instead of cosine-corrected irradiance could increase sensitivity of the technique while confining the field of view. However, we note that bloom-specific calibration of the NDI will be required until more is understood about the effects of chl *a* specific absorption coefficients, packaging effects, and light scatter on in situ ice algal spectral absorption.

No single environmental parameter fully explained the temporal variability in ice algal biomass. However, most of the variability was accounted for by a combination of the variables examined. Most notable was the influence of the warming ice cover (decreasing ice temperature gradient), which contributed to biomass loss through enhanced brine drainage as the interior ice eroded, increasing brine volume and thus brine-seawater exchange. Assessment of the vertical temperature gradient in sea ice also showed that an optimal temperature threshold for algal habitation of the bottom ice may exist. The negative effects of higher ice temperatures on ice algae biomass raise concerns about the impact of potentially warmer ice, resulting from rising air (Graversen et al., 2008; Jones et al., 2012) and ocean water temperatures caused by climate change (Steele et al., 2010), in the future Arctic.

Our approach to studying in situ relationships between ice algae and their environment emphasized the complexity of biophysical interactions in sea ice. At any one time during the bloom, algal biomass was subject to losses associated with under-ice currents that influenced bottom-ice erosion and melt. The influence of other variables changed in nature over the spring. These include habitat availability, which degraded in quality and availability with warming ice, and light intensity, which was limiting only during the time of snow cover. The interplay over the spring of these variables, along with others not examined in this study, such as nutrient availability and predation, make it difficult to predict bloom response to climate warming. However, they illustrate the need for additional integrated studies combined with modeling sensitivity analysis to make definitive conclusions on ice algal environmental controls.

ACKNOWLEDGEMENTS

This research was supported through a Northern Scientific Training Program grant to K. Campbell as well as funding from the Natural Sciences and Engineering Research Council of Canada, Canada Research Chairs program, and the Polar Continental Shelf Program of Natural Resources Canada. We would also like to thank Kristy Hugill, Virginie Galindo, Wayne Chan, Lauren Candlish, and Matt Gale for their contributions. This work is a contribution to the Canada Excellence Research Chair on Arctic Geomicrobiology and Centre for Earth Observation Science at the University of Manitoba, and ArcticNet.

REFERENCES

- Alou-Font, E., Mundy, C.J., Roy, S., Gosselin, M., and Agusti, S. 2013. Snow cover affects ice algae pigment composition in the coastal Arctic Ocean during spring. *Marine Ecology Progress Series* 474:89–104.
<http://dx.doi.org/10.3354/meps10107>
- Apollonio, S. 1965. Chlorophyll in Arctic sea-ice. *Arctic* 18(2):118–122.
<http://dx.doi.org/10.14430/arctic3457>
- Arrigo, K.R., Mock, T., and Lizotte, M.P. 2010. Primary producers and sea ice. In: Thomas, D.N., and Dieckmann, G.S., eds. *Sea ice*, 2nd ed. Oxford: Wiley Blackwell Publishing. 283–325.
<http://dx.doi.org/10.1002/9781444317145.ch8>
- Arrigo, K.R., Perovich, D.K., Pickart, R.S., Brown, Z.W., van Dijken, G.L., Lowry, K.E., Mills, M.M., et al. 2012. Massive phytoplankton blooms under Arctic sea ice. *Science* 336(6087):1408.
<http://dx.doi.org/10.1126/science.1215065>
- Belzile, C., Johannessen, S.C., Gosselin, M., Demers, S., and Miller, W.L. 2000. Ultraviolet attenuation by dissolved and particulate constituents of first-year ice during late spring in an Arctic polynya. *Limnology and Oceanography* 45(6):1265–1273.
<http://dx.doi.org/10.4319/lo.2000.45.6.1265>
- Blais, M., Gosselin, M., Mundy, C.J., Roy, S., Charette, J., and Tremblay, J.-É. 2012. Spotlight on sea ice algae: Influence of light on pigment composition of sea ice algae in Resolute (Nunavut) during spring 2010 and 2011. Poster presentation at the Québec-Océan Annual Meeting, 7–9 November 2012, Montréal, Québec.
- Bricaud, A., Claustre, H., Ras, J., and Oubelkheir, K. 2004. Natural variability of phytoplanktonic absorption in oceanic waters: Influence of the size structure of algal populations. *Journal of Geophysical Research* 109, C11010.
<http://dx.doi.org/10.1029/2004JC002419>
- Campbell, K., Mundy, C.J., Barber, D.G., and Gosselin, M. 2014. Characterizing the sea ice algae chlorophyll *a*–snow depth relationship over spring melt using transmitted irradiance. *Journal of Marine Systems*.
<http://dx.doi.org/10.1016/j.jmarsys.2014.01.008>
- Cota, G.F., and Horne, E.P.W. 1989. Physical control of Arctic ice algal production. *Marine Ecology Progress Series* 52:111–121.
<http://dx.doi.org/10.3354/meps052111>
- Cota, G.F., and Smith, R.E.H. 1991. Ecology of bottom ice algae: III. Comparative physiology. *Journal of Marine Systems* 2(3-4):297–315.
[http://dx.doi.org/10.1016/0924-7963\(91\)90038-V](http://dx.doi.org/10.1016/0924-7963(91)90038-V)
- Cota, G.F., Legendre, L., Gosselin, M., and Ingram, R.G. 1991. Ecology of bottom ice algae: 1. Environmental controls and variability. *Journal of Marine Systems* 2(3-4):257–277.
[http://dx.doi.org/10.1016/0924-7963\(91\)90036-T](http://dx.doi.org/10.1016/0924-7963(91)90036-T)
- Cox, G.F.N., and Weeks, W.F. 1983. Equations for determining the gas and brine volumes in sea-ice samples. *Journal of Glaciology* 29(102):306–316.
- Eicken, H. 1992. The role of sea ice in structuring Antarctic ecosystems. *Polar Biology* 12(1):3–13.
<http://dx.doi.org/10.1007/BF00239960>
- Fortier, M., Fortier, L., Michel, C., and Legendre, L. 2002. Climatic and biological forcing of the vertical flux of biogenic particles under seasonal Arctic sea ice. *Marine Ecology Progress Series* 225:1–16.
<http://dx.doi.org/10.3354/meps225001>
- Garrison, D.L., and Buck, K.R. 1986. Organism losses during ice melting: A serious bias in sea ice community studies. *Polar Biology* 6(4):237–239.
<http://dx.doi.org/10.1007/BF00443401>
- Golden, K.M., Ackley, S.F., and Lytle, V.I. 1998. The percolation phase transition in sea ice. *Science* 282(5397):2238–2241.
<http://dx.doi.org/10.1126/science.282.5397.2238>
- Gosselin, M., Legendre, L., Demers, S., and Ingram, R.G. 1985. Responses of sea-ice microalgae to climatic and fortnightly tidal energy inputs (Manitounuk Sound, Hudson Bay). *Canadian Journal of Fisheries and Aquatic Sciences* 42(5):999–1006.
<http://dx.doi.org/10.1139/f85-125>
- Gosselin, M., Legendre, L., Therriault, J.-C., Demers, S., and Rochet, M. 1986. Physical control of the horizontal patchiness of sea-ice microalgae. *Marine Ecology Progress Series* 29:289–298.
<http://dx.doi.org/10.3354/meps029289>
- Gosselin, M., Legendre, L., Therriault, J.-C., and Demers, S. 1990. Light and nutrient limitation of sea-ice microalgae (Hudson Bay, Canadian Arctic). *Journal of Phycology* 26(2):220–232.
<http://dx.doi.org/10.1111/j.0022-3646.1990.00220.x>
- Gotelli, N.J., and Ellison, A.M. 2004. *A primer of ecological statistics*. Sunderland, Massachusetts: Sinauer Associates, Inc.
- Gradinger, R., Spindler, M., and Henschel, D. 1991. Development of Arctic sea-ice organisms under graded snow cover. In: Sakshaug, E., Hopkins, C.C.E., and Øritsland, N.A., eds. *Proceedings of the Pro Mare Symposium on Polar Marine Ecology*, Trondheim, Norway, 12–16 May 1990. *Polar Research* 10(1):295–307.
- Graversen, R.G., Mauritsen, T., Tjernström, M., Källén, E., and Svensson, G. 2008. Vertical structure of recent Arctic warming. *Nature* 451:53–57.
<http://dx.doi.org/10.1038/nature06502>
- Holm-Hansen, O., Lorenzen, C.J., Holmes, R.W., and Strickland, J.D.H. 1965. Fluorometric determination of chlorophyll. *ICES Journal of Marine Science* 30(1):3–15.
<http://dx.doi.org/10.1093/icesjms/30.1.3>
- Horner, R., and Schrader, G.C. 1982. Relative contributions of ice algae, phytoplankton, and benthic microalgae to primary production in nearshore regions of the Beaufort Sea. *Arctic* 35(4):485–503.
<http://dx.doi.org/10.14430/arctic2356>
- Horner, R., Ackley, S.F., Dieckmann, G.S., Gulliksen, B., Hoshiai, T., Legendre, L., Melnikov, I.A., Reeburgh, W.S., Spindler, M., and Sullivan, C.W. 1992. Ecology of sea ice biota I. Habitat, terminology, and methodology. *Polar Biology* 12(3-4):417–427.
<http://dx.doi.org/10.1007/BF00243113>
- Hsiao, S.I.C. 1992. Dynamics of ice algae and phytoplankton in Frobisher Bay. *Polar Biology* 12:645–651.
<http://dx.doi.org/10.1007/BF00236987>

- Iacozza, J., and Barber, D.G. 1999. An examination of the distribution of snow on sea ice. *Atmosphere-Ocean* 37(1):21–51.
<http://dx.doi.org/10.1080/07055900.1999.9649620>
- Jones, P.D., Lister, D.H., Osborn, T.J., Harpham, C., Salmon, M., and Morice, C.P. 2012. Hemispheric and large-scale land-surface air temperature variations: An extensive revision and an update to 2010. *Journal of Geophysical Research* 117, D05127.
<http://dx.doi.org/10.1029/2011JD017139>
- Juhl, A.R., and Krembs, C. 2010. Effects of snow removal and algal photoacclimation on growth and export of ice algae. *Polar Biology* 33(8):1057–1065.
<http://dx.doi.org/10.1007/s00300-010-0784-1>
- Lavoie, D., Denman, K., and Michel, C. 2005. Modeling ice algal growth and decline in a seasonally ice-covered region of the Arctic (Resolute Passage, Canadian Archipelago). *Journal of Geophysical Research* 110, C11009.
<http://dx.doi.org/10.1029/2005JC002922>
- Legendre, L., and Gosselin, M. 1991. In situ spectroradiometric estimation of microalgal biomass in first-year sea ice. *Polar Biology* 11(2):113–115.
<http://dx.doi.org/10.1007/BF00234273>
- Legendre, L., Aota, M., Shirasawa, K., Martineau, M.-J., and Ishikawa, M. 1991. Crystallographic structure of sea ice along a salinity gradient and environmental control of microalgae in the brine cells. *Journal of Marine Systems* 2(3-4):347–357.
[http://dx.doi.org/10.1016/0924-7963\(91\)90041-R](http://dx.doi.org/10.1016/0924-7963(91)90041-R)
- Legendre, L., Ackley, S.F., Dieckmann, G.S., Gulliksen, B., Horner, R., Hoshiai, T., Melnikov, I.A., Reeburgh, W.S., Spindler, M., and Sullivan, C.W. 1992. Ecology of sea ice biota 2. Global significance. *Polar Biology* 12(3-4):429–444.
<http://dx.doi.org/10.1007/BF00243114>
- Leu, E., Søreide, J.E., Hessen, D.O., Falk-Peterson, S., and Berge, J. 2011. Consequences of changing sea-ice cover for primary and secondary producers in the European Arctic shelf seas: Timing, quantity, and quality. *Progress in Oceanography* 90(1-4):18–32.
<http://dx.doi.org/10.1016/j.pocean.2011.02.004>
- Marsden, R.F., Paquet, R., and Ingram, R.G. 1994. Currents under land-fast ice in the Canadian Arctic Archipelago Part I: Vertical velocities. *Journal of Marine Research* 52(6):1017–1036.
- Maykut, G.A., and Grenfell, T.C. 1975. The spectral distribution of light beneath first-year sea ice in the Arctic Ocean. *Limnology and Oceanography* 20(4):554–563.
<http://dx.doi.org/10.4319/lo.1975.20.4.0554>
- Michel, C., Legendre, L., Ingram, R.G., Gosselin, M., and Lavoie, D. 1996. Carbon budget of sea-ice algae in spring: Evidence of a significant transfer to zooplankton grazers. *Journal of Geophysical Research* 101(C8):18345–18360.
<http://dx.doi.org/10.1029/96JC00045>
- Michel, C., Ingram, R.G., and Harris, L.R. 2006. Variability in oceanographic and ecological processes in the Canadian Arctic Archipelago. *Progress in Oceanography* 71(2-4):379–401.
<http://dx.doi.org/10.1016/j.pocean.2006.09.006>
- Morgan-Kiss, R., Ivanov, A.G., Williams, J., Mobashsher, K., and Huner, N.P. 2002. Differential thermal effects on the energy distribution between photosystem II and photosystem I in thylakoid membranes of a psychrophilic and a mesophilic alga. *Biochimica et Biophysica Acta* 1561(2):251–265.
- Morgan-Kiss, R.M., Priscu, J.C., Pockock, T., Gudynaite-Savitch, L., and Huner, N.P.A. 2006. Adaptation and acclimation of photosynthetic microorganisms to permanently cold environments. *Microbiology and Molecular Biology Reviews* 70(1):222–252.
<http://dx.doi.org/10.1128/MMBR.70.1.222-252.2006>
- Mundy, C.J., Barber, D.G., and Michel, C. 2005. Variability of snow and ice thermal, physical and optical properties pertinent to sea ice biomass during spring. *Journal of Marine Systems* 58(3-4):107–120.
<http://dx.doi.org/10.1016/j.jmarsys.2005.07.003>
- Mundy, C.J., Barber, D.G., Michel, C., and Marsden, R.F. 2007a. Linking ice structure and microscale variability of algal biomass in Arctic first-year sea ice using an in situ photographic technique. *Polar Biology* 30(9):1099–1114.
<http://dx.doi.org/10.1007/s00300-007-0267-1>
- Mundy, C.J., Ehn, J.K., Barber, D.G., and Michel, C. 2007b. Influence of snow cover and algae on the spectral dependence of transmitted irradiance through Arctic landfast first-year sea ice. *Journal of Geophysical Research* 112, C03007.
<http://dx.doi.org/10.1029/2006JC003683>
- Mundy, C.J., Gosselin, M., Ehn, J., Gratton, Y., Rossnagel, A., Barber, D.G., Martin, J., et al. 2009. Contribution of under-ice primary production to an ice-edge upwelling phytoplankton bloom in the Canadian Beaufort Sea. *Geophysical Research Letters* 36, L17601.
<http://dx.doi.org/10.1029/2009GL038837>
- Parsons, T.R., Maita, Y., and Lalli, C.M. 1984. A manual of chemical and biological methods for seawater analysis. New York: Pergamon Press.
- Perovich, D.K. 1996. The optical properties of sea ice. Monograph 96-1. Hanover, New Hampshire: U.S. Army Corps of Engineers, Cold Regions Research & Engineering Laboratory. 23 p.
- Perovich, D.K., Roesler, C.S., and Pegau, W.S. 1998. Variability in Arctic sea ice optical properties. *Journal of Geophysical Research* 103(C1):1193–1208.
<http://dx.doi.org/10.1029/97JC01614>
- Pielou, E.C. 1984. The interpretation of ecological data: A primer on classification and ordination. New York: Wiley.
- Polashenski, C., Perovich, D., and Courville, Z. 2012. The mechanisms of sea ice melt pond formation and evolution. *Journal of Geophysical Research* 117, C01001.
<http://dx.doi.org/10.1029/2011JC007231>
- Pringle, D.J., Miner, J.E., Eicken, H., and Golden, K.M. 2009. Pore space percolation in sea ice single crystals. *Journal of Geophysical Research* 117, C12017.
<http://dx.doi.org/10.1029/2008JC005145>
- Rintala, J.-M., Piiparinen, J., Ehn, J., Autio, R., and Kuosa, H. 2006. Changes in phytoplankton biomass and nutrient quantities in sea ice as responses to light/dark manipulations during different phases on the Baltic winter 2003. *Hydrobiologia* 554:11–24.
<http://dx.doi.org/10.1007/s10750-005-1002-y>

- Robinson, D.H., Arrigo, K.R., Iturriaga, R., and Sullivan, C.W. 1995. Microalgal light-harvesting in extreme low-light environments in McMurdo Sound, Antarctica. *Journal of Phycology* 31(4):508–520.
<http://dx.doi.org/10.1111/j.1529-8817.1995.tb02544.x>
- Rózanska, M., Gosselin, M., Poulin, M., Wiktor, J.M., and Michel, C. 2009. Influence of environmental factors on the development of bottom ice protist communities during the winter–spring transition. *Marine Ecology Progress Series* 386:43–59.
<http://dx.doi.org/10.3354/meps08092>
- Smith, R.E.H., Anning, J., Clement, P., and Cota, G. 1988. Abundance and production of ice algae in Resolute Passage, Canadian Arctic. *Marine Ecology Progress Series* 48:251–263.
- Smith, R.E.H., Harrison, W.G., Harris, L.R., and Herman, A.W. 1990. Vertical fine structure of particulate matter and nutrients in sea ice of the High Arctic. *Canadian Journal of Fisheries and Aquatic Sciences* 47(7):1348–1355.
- SooHoo, J.B., Palmisano, A.C., Kottmeier, S.T., Lizotte, M.P., SooHoo, S.L., and Sullivan, C.W. 1987. Spectral light absorption and quantum yield of photosynthesis in sea ice microalgae and a bloom of *Phaeocystis pouchetii* from McMurdo Sound, Antarctica. *Marine Ecology Progress Series* 39:175–189.
<http://dx.doi.org/10.3354/meps039175>
- Søreide, J.E., Leu, E., Berge, J., Graeve, M., and Falk-Petersen, S. 2010. Timing of blooms, algal food quality and *Calanus glacialis* reproduction and growth in a changing Arctic. *Global Change Biology* 16(11):3154–3163.
<http://dx.doi.org/10.1111/j.1365-2486.2010.02175.x>
- Steele, M., Zhang, J., and Ermold, W. 2010. Mechanisms of summertime upper Arctic Ocean warming and the effect on sea ice melt. *Journal of Geophysical Research* 115, C11004.
<http://dx.doi.org/10.1029/2009JC005849>
- Welch, H.E., and Bergmann, M.A. 1989. Seasonal development of ice algae and its prediction from environmental factors near Resolute, N.W.T., Canada. *Canadian Journal of Fisheries and Aquatic Sciences* 46(10):1793–1804.
<http://dx.doi.org/10.1139/f89-227>
- Welch, H.E., Bergmann, M.A., Jorgenson, J.K., and Burton, W. 1988. A subice suction corer for sampling epontic ice algae. *Canadian Journal of Fisheries and Aquatic Sciences* 45(3):562–568.
<http://dx.doi.org/10.1139/f88-067>